The Astrophysical Journal, 600:1035–1042, 2004 January 10
© 2004. The American Astronomical Society. All rights reserved. Printed in U.S.A.

KINEMATIC TREATMENT OF CORONAL MASS EJECTION EVOLUTION IN THE SOLAR WIND

Pete Riley
Science Applications International Corporation, San Diego, CA 92121; pete.riley@saic.com

and

N. U. Crooker
Center for Space Physics, Boston University, 725 Commonwealth Avenue, Boston, MA 02215; crooker@bu.edu
Received 2003 July 15; accepted 2003 September 24

ABSTRACT

We present a kinematic study of the evolution of coronal mass ejections (CMEs) in the solar wind. Specifically, we consider the effects of (1) spherical expansion and (2) uniform expansion due to pressure gradients between the interplanetary CME (ICME) and the ambient solar wind. We compare these results with an MHD model that allows us to isolate these effects from the combined kinematic and dynamical effects, which are included in MHD models. They also provide compelling evidence that the fundamental cross section of so-called "force-free" flux ropes (or magnetic clouds) is neither circular or elliptical, but rather a convex-outward, "pancake" shape. We apply a force-free fit to the magnetic vectors from the MHD simulation to assess how the distortion of the flux rope affects the fit. In spite of these limitations, force-free fits, which are straightforward to apply, do provide an important description of a number of parameters, including the radial dimension, orientation, and chirality of the ICME.

Subject headings: MHD — solar wind — Sun: activity — Sun: corona — Sun: coronal mass ejections (CMEs) — Sun: magnetic fields

On-line material: color figures

1. INTRODUCTION

Magnetic clouds (MCs) or flux ropes (we do not distinguish between the two terms here) are transient solar wind structures characterized by (1) strong magnetic fields, (2) large coherent rotations in the magnetic field vector, and (3) low proton temperature (Burlaga et al. 1981). Since their discovery in solar wind data more than 20 years ago, they have been a major focus of heliospheric research. The commonly held view is that they represent the simplest—or perhaps most pristine—example of a more general class of interplanetary coronal mass ejections (ICMEs). However, we emphasize that the theoretical relationship between ICMEs and MCs is not well understood.

A simple, yet successful, technique for modeling flux ropes in the solar wind is the so-called force-free model (e.g., Burlaga 1988; Lepping, Jones, & Burlaga 1990; Marubashi 1997; Mulligan et al. 2001; Hidalgo et al. 2002a). In its early inception, clouds were envisaged to have cylindrically symmetric force-free configurations (e.g., Burlaga 1988) and solutions of $\nabla \times \boldsymbol{B} = \alpha \boldsymbol{B}$ involving Bessel functions of the first kind (Lundquist 1950) yielded profiles for the magnetic field components that often matched observations well. Recent extensions to this have considered (1) cloud expansion via ad hoc modifications to the model field components (e.g., Marubashi 1997), (2) multi-spacecraft observations (e.g., Mulligan et al. 2001), (3) including two radii of curvature—one for the flux rope cross section and one for the curvature of the rope axis, (4) non–force-free effects by fitting to current densities (Hidalgo et al. 2002a), and (5) elliptical cross sections (Hidalgo, Nieves-Chinchilla, & Cid 2002b; Russell & Mulligan 2002).

An alternative approach for determining the properties of magnetic flux ropes has been developed recently by Hu & Sonnerup (2002). Using magnetic field and plasma measurements, they are able to estimate a number of parameters characterizing the flux rope, including its orientation, impact parameter, size, maximum field strength, and twist by integrating the nonlinear, plane Grad-Shafranov equation. What is particularly appealing about this technique, as it pertains to the present study, is that it allows one to reconstruct the global structure of the cloud in the plane perpendicular to the cloud's axis. So far, only three events have been analyzed, including a double flux rope (Hu & Sonnerup 2002; Hu et al. 2003).

The success of the force-free models has led to a view of MCs as locally cylindrically symmetric flux ropes that may or may not be connected back to the Sun. This is summarized by the illustrations shown in Figures 1*a*–1*c*. Extensions to this picture have included the effects of solar rotation (Fig. 1*d*), and dynamical effects resulting from fast CMEs ploughing into ambient solar wind ahead and "flattening" (Fig. 1*e*). *Ulysses*, while immersed in continuous fast, quiescent coronal hole flow, observed a distinct set of CME-related signatures, which led Gosling et al. (1994) to propose the picture shown in Figure 1*f*.

Fluid and MHD models have also been developed to explore the initiation (e.g., Mikić & Linker 1994; Linker & Mikić 1997 Antiochos, Devore, & Klimchuk 1999; Lin et al. 1998 Titov & Demoulin 1999; Filippov, Gopalswamy, & Lozhechkin 2001) and evolution (e.g., Riley, Gosling, & Pizzo 1997; Riley & Gosling 1998; Riley et al. 2002, 2003; Odstrcil et al. 2002; Vandas, Odstrcil, & Watari 2002; Cargill & Schmidt 2002) of CMEs near the Sun and in the solar wind. These models include a rich variety of physics and have been quite successful in reproducing a wide range of observational signatures. However, as the level of sophistication in the model increases, so to does the difficulty in interpreting the results. In particular, it can be difficult to distinguish between competing processes.

Previous studies have considered some aspects of kinematic distortion. Newkirk, Hundhausen, & Pizzo (1981), for example, considered the temporal evolution of "bubble"-shaped structures, illustrating primarily the azimuthal elongation of the bubble and distortion in response to fast and slow solar wind

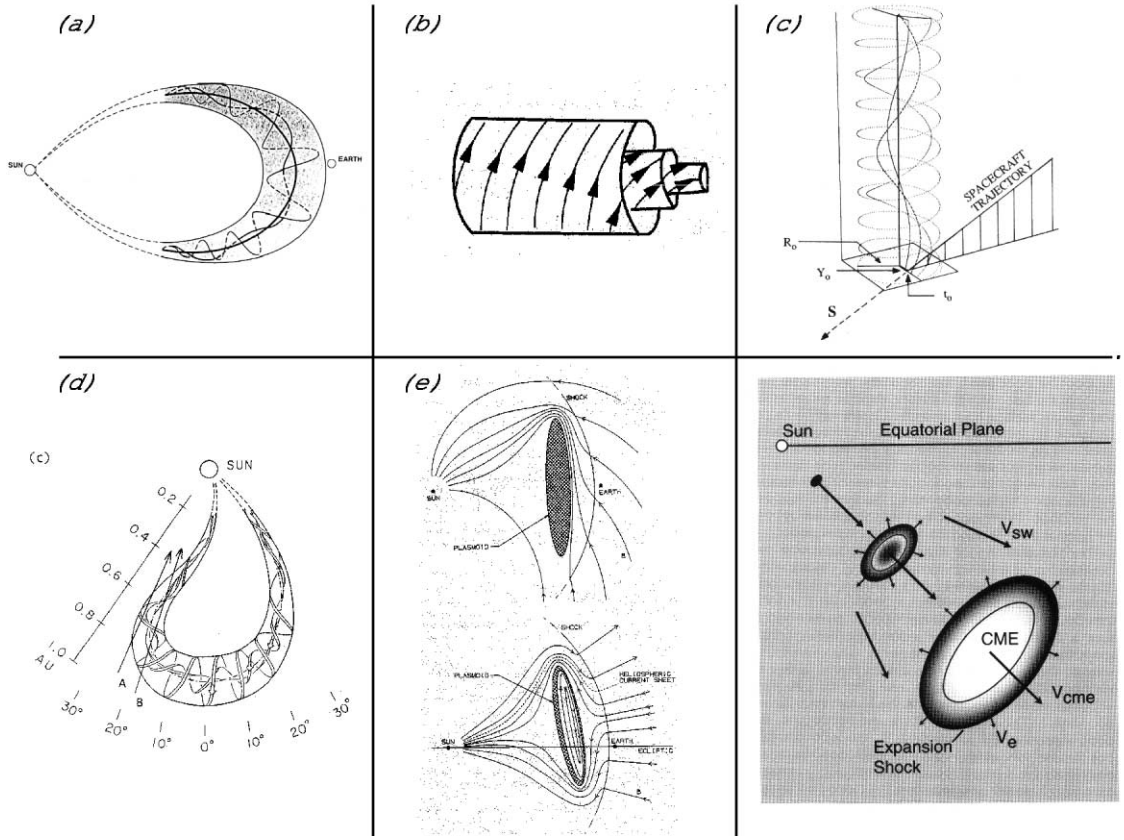

FIG. 1.—Illustrative collection of flux rope schematics, highlighting different aspects of the properties and evolution of ICMEs. (*a*) Global profile of a magnetic cloud approaching 1 AU (Burlaga, Lepping, & Jones 1990); (*b*) Helical properties of cylindrical flux rope field lines (Bothmer & Schwenn 1998); (*c*) Spacecraft trajectory through a cylindrical flux rope (Lepping et al. 1990); (*d*) Global picture of flux rope approaching 1 AU, including the effects of solar rotation (Marubashi 1997); (*e*) Dynamical effects on evolution of a fast CME (Gosling 1990); and (*f*) Schematic of CME evolution at high heliographic latitudes (Gosling et al. 1994).

streams. Suess (1988) described the basic kinematic deformation of an initially circular cross section as it convected away from the Sun in a spherically expanding solar wind. However, by adopting the prevalent view that the cross section of magnetic clouds was approximately circular, he reasoned that magnetic tension must be sufficiently strong to resist such a distortion. He further suggested that the observed radial expansion often seen in magnetic clouds could then be produced by the clouds tendency to minimize departures from force-free equilibrium brought about by spherical expansion.

Multi-spacecraft observations of the same magnetic cloud offer an opportunity to infer a more global picture. Crooker & Intriligator (1996), for example, analyzed a magnetic cloud observed by two spacecraft, the *Interplanetary Monitoring Platform (IMP) 8* at Earth and *Pioneer 11* at 4.8 AU. The longitudinal separation of the two spacecraft was 30°, and their observations clearly indicated a distention of the ejecta. On the other hand, the observed declining speed profiles at the two spacecraft suggested that radial expansion had taken place, at least, close to the Sun. Thus they concluded that, in addition to kinematic distortion, dynamic expansion must have also taken place. Riley et al. (2003) studied a magnetic cloud observed by the *Advanced Composition Explorer (ACE)* at 1 AU and in the ecliptic plane and by *Ulysses* at 5 AU and S22° heliographic latitude. In conjunction with an MHD simulation, they derived a global picture of the event as it must have looked crossing the two spacecraft, consisting of a flattened, convex-outward ejecta in which the transverse dimensions were significantly larger than the radial dimension.

In this paper, we analyze the propagation and evolution of flux rope CMEs using a kinematic approach. Our purpose is to show that, using the simplest technique possible, the most basic shape of a flux rope CME in the solar wind is not cylindrical but rather a convex-outward, "pancake" shape. Such a technique, while highly idealized, bridges the gap between the simple force-free models and the more complex numerical MHD models. Although we describe the evolution of the flux ropes in terms of their magnetic field, the results apply equally well to non–flux rope CMEs. Our goals are to isolate nondynamical effects from the MHD solutions and describe the fundamental cross sectional structure that we believe should be incorporated into future force-free and non–force-free flux rope fitting models. The prevalent view that force-free flux ropes (and ICMEs in general) are cylindrical structures is unlikely to be met in most, if not all cases, implying that the illustrations collected in Figure 1 are incorrect, even at the schematic level.

2. KINEMATIC EVOLUTION

To model the kinematic evolution of magnetic flux ropes in the solar wind (where we use the term "solar wind" to refer to everything above the solar surface), we consider an initially circular flux rope configuration, centered 1 R_S above the solar surface, with an initial radius of 1 R_S (Fig. 2*a*). Because of the implied symmetry in the azimuthal direction, by extension, this is a torus in three dimensions, and thus "field lines" close back on themselves and not back to the Sun. (Note that to be considered "cylindrical" would require that the radius of the

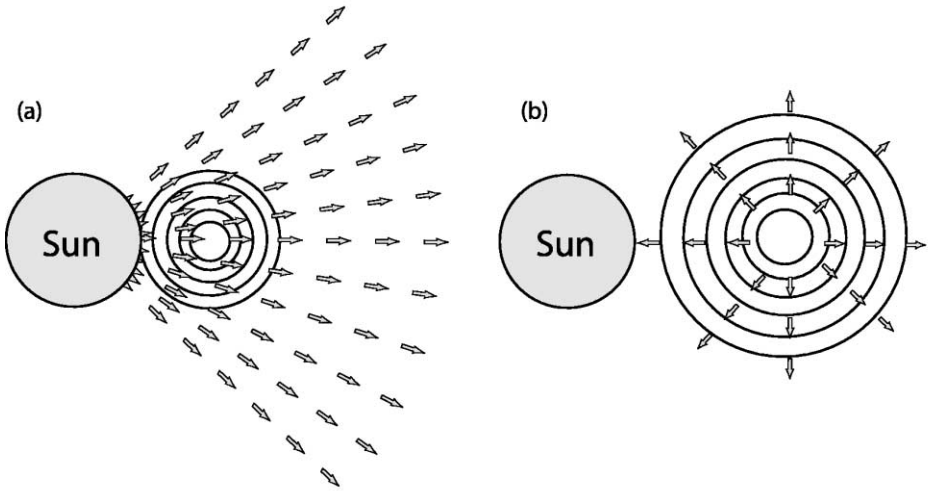

FIG. 2.—Kinematic effects on evolution of magnetic flux rope. (*a*) Convective evolution or spherical expansion; and (*b*) expansion of the flux rope caused by a pressure gradient between it and the ambient solar wind. [*See the electronic edition of the Journal for a color version of this figure.*]

flux rope $r_{\rm fluxrope} \ll 1\ R_S$). Although highly idealized, numerous observations of CMEs launched off the solar limb suggest that such a shape is a reasonable starting point. We consider two types of kinematic evolution: (1) spherical expansion due to simple convection with the ambient solar wind in a diverging geometry and (2) expansion due to a uniform pressure gradient between the flux rope and the ambient solar wind. The first effect is a true kinematic process, whereas the second is a dynamic process that we are treating kinematically. These two effects are shown in Figures 2*a* and 2*b*, respectively. Modeling the convective evolution involves nothing more than tracking the loci of a set of points in a uniform spherical expansion. We assume purely radial flow so that the points maintain constant latitude but move outward by a distance $\Delta R = v_r \Delta t$, where Δt is some arbitrary time step and v_r is the velocity of the solar wind. Expansion due to a pressure gradient between the CME and the ambient solar wind can be implemented kinematically by calculating the unit outward normal to the CME boundary (i.e., the direction of $-\nabla P$, assuming the pressure of the flux rope is higher than that of the surrounding medium so that it expands rather than collapses) and shifting it by some constant value (i.e., $\Delta \boldsymbol{R} = \boldsymbol{v}^{\rm exp} \Delta t = (i/n) v_0^{\rm exp} \Delta t \boldsymbol{e}_\perp$), where $v_0^{\rm exp}$ is some arbitrary constant expansion speed, n is the number of concentric circles that make up the flux rope, and i is the index of the circle under consideration. Thus the factor i/N reflects the fact that pressure gradient expansion is smallest near the center of the flux rope and largest at the edge. Note that a circle will maintain its shape under this operation, however, a more complex structure will deform.

Practically, these ideas are easily incorporated into a simple computer program using a combination of translations, numerical derivatives, and transformations between Cartesian and polar coordinates. We apply these operations to a set of concentric circles (as illustrated in Fig. 2) to mimic the evolution of the poloidal component of the magnetic field within the flux rope.

3. RESULTS

We consider first the effects of spherical expansion (i.e., convective evolution) alone on the flux rope. Figure 3 summarizes the evolution of an initially cylindrical flux rope at various heliocentric distances. Initially, the effect of the diverging spherical geometry is to flatten the trailing edge of the flux rope. Later on the flux rope develops a convex-outward, "pancake" shape. This is simply the result of the spherical geometry of the system and is not related to any interaction between the flux rope and the ambient wind (since there is none). The initial radial width of the flux rope was 1 R_S, and it remains this value throughout its evolution. By 1 AU (215 R_S), the flux rope's transverse dimension dominates its radial width and it has the appearance of being "smeared" over a circular arc. The angular span of the flux rope remains a constant 60°.

Observed MCs have a typical radial width of $\sim$0.25 AU at 1 AU (Burlaga 1988), and so spherical expansion alone cannot produce such dimensions given their initial radial extent at the Sun. At the Sun, white light observations suggest that CMEs are undergoing strong expansion because of a higher internal pressure. In the solar wind, in situ observations often show declining speed profiles within ICMEs, demonstrating that they are continuing to expand. However, where this expansion is most significant is not well known. Thus, for simplicity, in our analysis we assume a linear expansion as a function of time. As we will see, comparison with MHD results suggests that this is a reasonable approximation to make. It is important to note that while successive operations of spherical expansion are commutative, mixing pressure gradient expansion with spherical expansion is not. This is a consequence of the fact that the direction of the pressure gradient expansion is along the normal to the boundary of the flux rope, which is a function of time. Thus we evolve the flux rope by performing a repeated sequence of spherical expansion followed by pressure gradient expansion.

Figure 4 illustrates these effects on our idealized flux rope. We chose the pressure gradient expansion velocity to be such that a radial width of approximately $\sim$0.25 AU was produced at 1 AU. As in the previous case, the initial response of the flux rope to the spherical expansion is seen as a flattening of the trailing edge. At 3 R_S the aspect ratio (defined to be the ratio of the latitudinal extent of the flux rope to its radial extent at the equator) is 1.4. By 30 R_S, however, the effects of pressure gradient expansion can be clearly seen in increased radial width of the flux rope ($\sim$8 R_S) and an aspect ratio of 5.1. At 108 R_S, the aspect ratio has risen to 6.7. By 1 AU, the flux rope extends

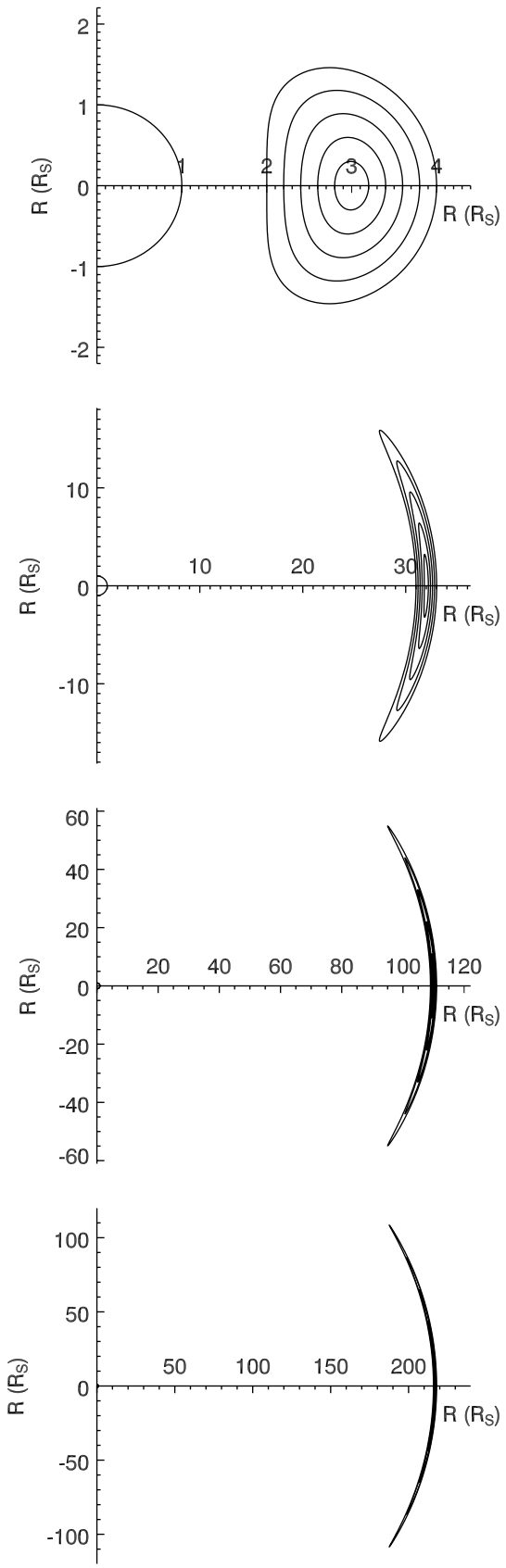

FIG. 3.—Evolution of a flux rope due only to the effects of spherical expansion. Shown are snapshots of the flux rope at $\sim$3, 32, 110, and 215 R_S.

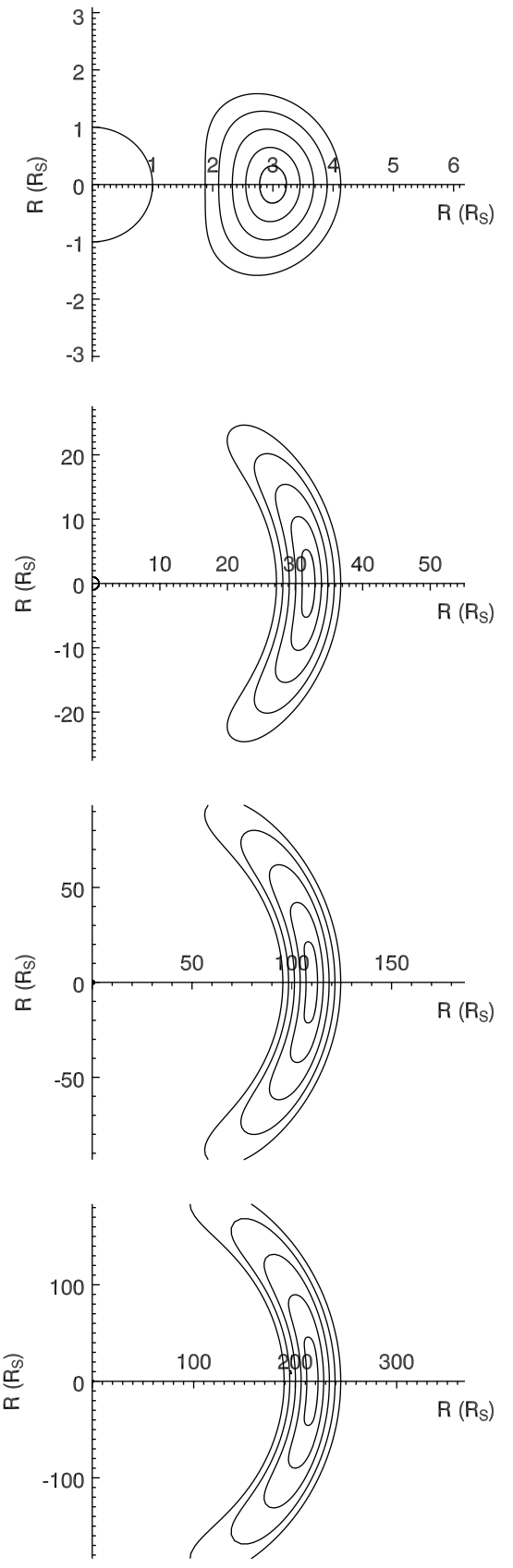

FIG. 4.—Evolution of a flux rope due to the effects of both spherical expansion and pressure gradient expansion. Shown are snapshots of the flux rope at $\sim$3, 32, 110, and 215 R_S.

$\sim$55 R_S ($\sim$0.25 AU) in the radial direction and $\sim$200 R_S out of the equatorial plane, leading to an aspect ratio of 5:1. We can also look at the angular span of the ejecta. For the four snapshots shown in Figure 4, from top to bottom, they were 66°, 98°, 114°, and 126°, respectively. This variation is due entirely to the pressure gradient expansion.

4. COMPARISON WITH AN MHD SIMULATION

We have developed a global MHD model of CME eruption at the Sun and evolution in the solar wind out to 5 AU (Odstrcil et al. 2002). Although idealized, we have found that the simulation reproduces many generic features of magnetic clouds (Riley et al. 2003), as well as predicting the presence of new phenomena that can be identified with in situ data (Riley et al. 2002). In Figure 5, we summarize the evolution of the flux rope at various times following its eruption. The radial lines indicate the latitudinal extent of the flux rope. A detailed description of these results has been presented elsewhere (Riley et al. 2002, 2003) and we restrict ourselves here to a brief description of the latitudinal and radial evolution of the flux rope. Comparison of these profiles with the kinematic evolution summarized in Figure 3 suggests that the two effects of spherical expansion and pressure gradient expansion dominate the evolution of the large-scale structure of the flux rope. The major difference between the two profiles is due to the presence of the heliospheric plasma sheet, a region of slower, denser plasma in this case offset from the equatorial plane by $-10°$, which has the effect of squeezing the ejecta. This highlights that in reality, the presence of a more highly structured ambient solar wind will play a significant role in distorting the flux rope beyond the concepts discussed here. Defining the aspect ratio to be the ratio of the maximum vertical extent of the ejecta to its radial extent in the equatorial plane, we find it to be 1.0, 3.1, 5.8, and 9.3 for the four snapshots

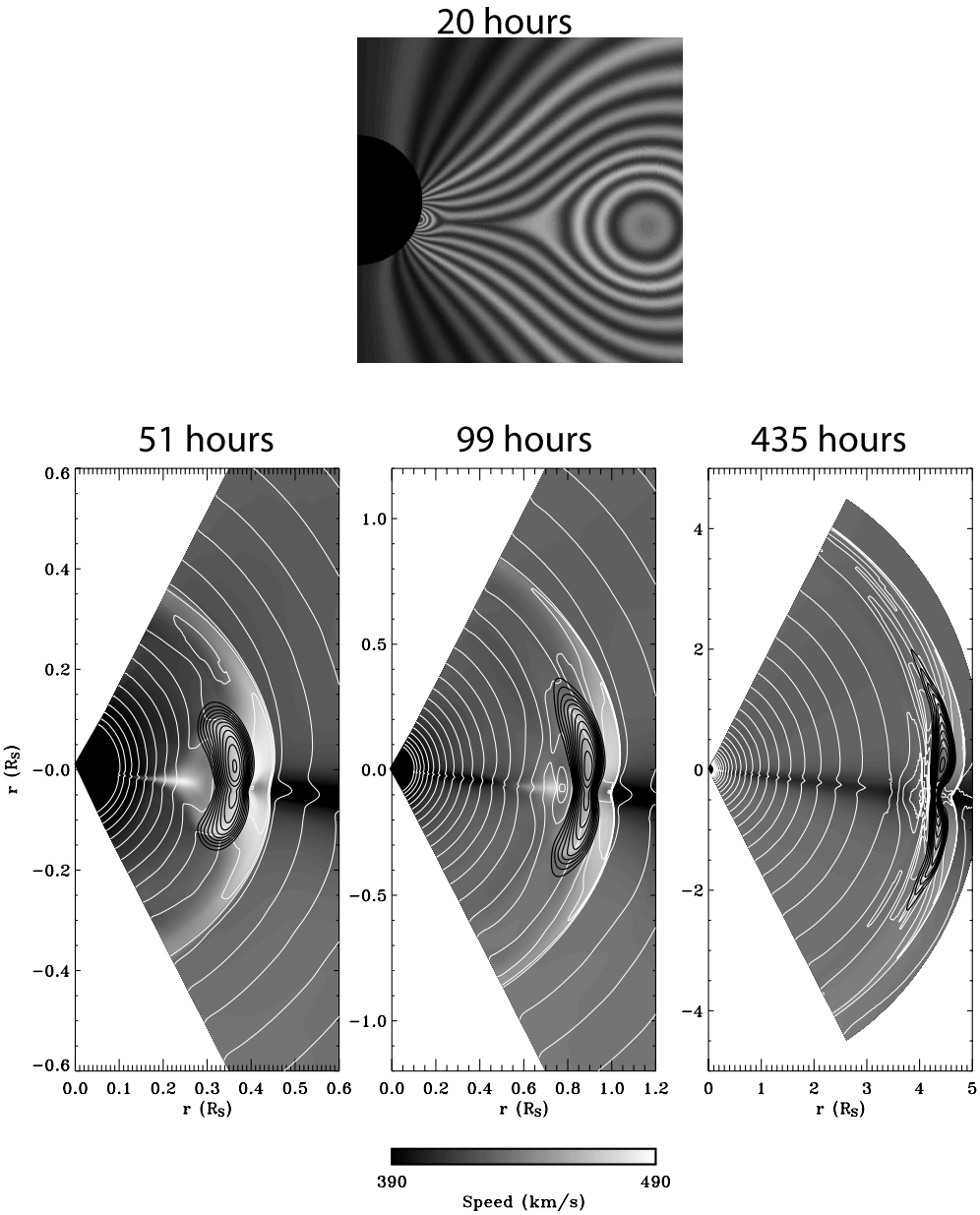

FIG. 5.—Radial velocity (*shaded contours*), magnetic flux function (*black, closed contours*), and number density (*white contours*) for three times during an MHD calculation. [*See the electronic edition of the Journal for a color version of this figure.*]

shown in Figure 5. Obviously, these values are quite sensitive to the particular latitude chosen. Nevertheless, the variation from one time to the next is not. Thus, the trend toward higher aspect ratios with increasing heliocentric distance is a real effect. We can also compute the angular span of the ejecta. Since the flux rope was not ejected exactly along the equatorial plane but displaced southward by $\sim 10^{\circ}$ or so, we have computed the angle $\theta = 2 \times \tan^{-1}(\Delta y/\Delta x)$, where Δy is the vertical span of the flux rope and Δx is the horizontal span of the ejecta. These values are 28°, 47°, 56°, and 59° for the four snapshots. Again, these numbers are not meant to be used for detailed quantitative analysis; it is their variation that primarily concerns us. We note that there is substantial angular expansion between 20 and 51 hr, when the flux rope moved from $\sim 4.7\ R_S$ to ~ 0.35 AU. This expansion had slowed by 99 hr (~ 0.9 AU) and still further by 435 hr (~ 4.4 AU).

We can apply force-free model fits to these simulation results by generating time series profiles at specific locations to mimic in situ measurements. In Figure 6 we compare such profiles with a force-free fit to the model data. The top three panels show speed, number density (n_p), and temperature (T_p) as a function of time. The hypothetical spacecraft was located at 2°N heliographic latitude and 5 AU from the Sun. The boundaries of the flux rope are indicated by the vertical lines. The declining speed profile within the flux rope indicates that the structure is expanding. This is supported by the low density and temperature within the ejecta. It is also driving a fast forward shock, standing almost 1 day ahead of the leading edge of the flux rope. The remaining four panels summarize the magnetic field components as well as the magnitude of the field. They are shown in the *rtn* coordinate system where $\boldsymbol{e}_r$ is the radial direction (positive is away from the Sun), $\boldsymbol{e}_t$ is parallel to the equatorial plane and in the direction of planetary motion, and $\boldsymbol{e}_n$ completes the right-handed system. (Relative to the more familiar spherical coordinate system (r,θ,ϕ), $\boldsymbol{e}_t = \boldsymbol{e}_\phi$ and $\boldsymbol{e}_n = -\boldsymbol{e}_\theta$.) The simulated magnetic components show the classic features of a magnetic cloud with its axis lying parallel to the equatorial plane and perpendicular to the radial direction: the radial component of the field remains zero throughout, the azimuthal component rotates from zero through to a maximum and back to zero, while the meridional component falls from a maximum through zero to a minimum negative value. The azimuthal component reflects changes in the axial component of the field and the meridional component reflects changes in the poloidal component. The force-free fitting technique we have applied follows that of Lepping et al. (1990) with the additional simplification that we know the precise orientation of the flux rope and so do not have to include these parameters in the fit. The magnitudes of the field components are set by the maximum value of the observed (or simulated in this case) axial field. Qualitatively, there is a fair agreement between the simulated profiles and the Bessel function fits. Notable exceptions are (1) the asymmetry present in the simulated profiles, (2) the larger extrema in the simulated B_n profiles, and (3) the relatively flat (but slightly declining) simulated magnetic field magnitude profile. The asymmetry is due primarily to the expansion of the ejecta, while the larger simulated B_n profile and flat/declining field magnitude profile are due to kinematic distortion.

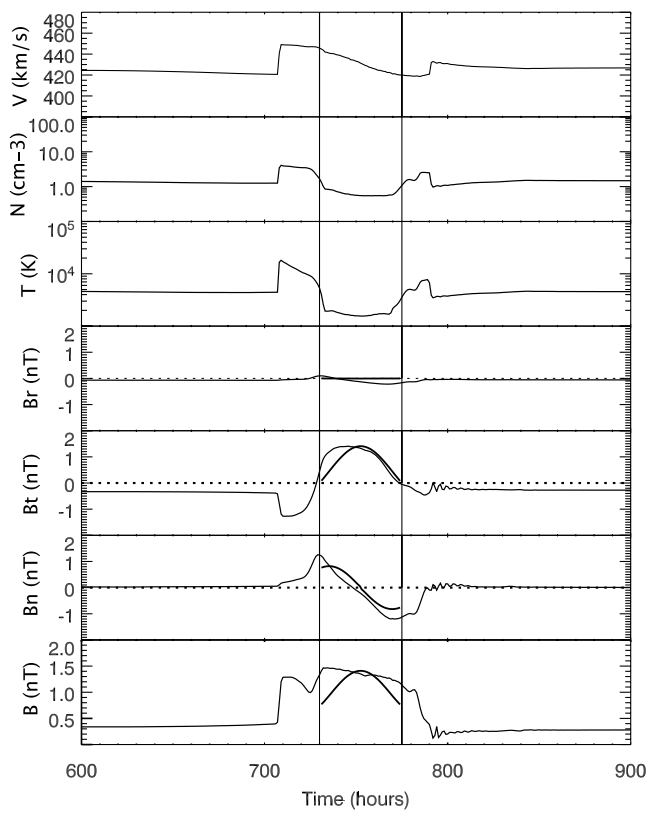

FIG. 6.—Comparison of MHD results with force-free fit to magnetic field parameters for the CME shown in Figure 5.

5. SUMMARY AND DISCUSSION

In this study, we have presented a kinematic study of the evolution of CMEs in the solar wind. By isolating the effects of spherical expansion and pressure gradient expansion and comparing the results with MHD simulations, we have been able to illustrate the importance of kinematic evolution on CME morphology.

One of the most important dynamical effects included in MHD simulations and not present in our kinematic analysis is due to the relative speed difference between the flux rope and the surrounding medium. CMEs are often launched with speeds significantly faster than the ambient solar wind, driving a forward wave, which eventually steepens into a shock and generates a region of enhanced pressure behind it (the sheath). The pressure gradients associated with this act to flatten the flux rope profile further on its leading edge. In contrast, in the region behind the flux rope, an expansion wave (rarefaction region) forms, accelerating the slower wind behind the flux rope and decelerating its trailing edge. This acts to resist the development of the convex-outward shape at the trailing edge. A second important effect—and one that we cannot address within the confines of the kinetic approach described here—concerns the properties of the ambient solar wind. At solar minimum, for example, when a band of slow, dense wind emanates from lower latitudes, while fast tenuous wind flows from large polar coronal holes, a CME initially launched into the slower wind will likely penetrate into the faster flow. The evolution of the flux rope in these two different environments will be fundamentally different, and the resulting global morphology of the flux rope will be significantly more complicated than suggested here (e.g., Riley et al. 1997). Magnetic reconnection at regions of strong velocity shear could further complicate the evolution of the CME by altering its initial topology (Schmidt & Cargill 2001).

Our kinematic examples show that when only spherical expansion is considered, the flux rope maintains constant

latitude ($\sim 30^\circ$ in the case shown in Figure 2). On the other hand, when pressure gradient expansion is added, the flux rope penetrates beyond $\sim 60^\circ$ latitude. In reality, the expansion associated with pressure gradients is unlikely to be a simple linear function of time as we have assumed. In fact, from Figure 5, we infer that in the panels from top to bottom right, the angular expansion progressed from 70% to 18% to 6%. Since the latitudinal extent of the flux rope is very sensitive to where this expansion takes place (because of the diverging geometry of the system), the true latitudinal extent may be substantially different, and our kinematic results should be taken as indicative but not quantitatively correct.

In our kinematic analysis, we have ignored any role played by magnetic tension in resisting the distortion of the cloud by spherical expansion (Suess 1988). This force, however, is included in the MHD model. Thus, the fact that the MHD simulations show the same qualitative distortions as the kinematic treatment suggests that magnetic tension does not provide a dominant restoring force. Moreover, for ICMEs that (1) do not contain well-defined flux ropes and/or (2) are not low-β structures, it is even more unlikely that tension plays a significant role in resisting distortion through spherical expansion. It has also been shown that magnetic tension provides very little resistance against strong velocity shear (Schmidt & Cargill 2001). Force-free models can, in principle, deduce the contribution played by magnetic tension. The differences between the fitted force-free profiles and the observed profiles provides a measure of the noncircularity of the poloidal component of the magnetic field. The asymmetry in the field magnitude in Figure 6 is largely due to the flattening of the ejecta. The effect is also seen in the meridional field component (B_n), for which the force-free model underestimates the field. The flattening effect of spherical expansion adds to the meridional component without affecting the maximum value of the axial field.

These kinematic distortions are a basic feature of all MCs. Cylindrical force-free models, including those that treat the effects of expansion along the trajectory of the spacecraft, may benefit greatly by incorporating the effects of the evolution described here. One way to accomplish this would be to add an "aspect ratio" free parameter into the fitting technique. This might be defined as the ratio of the semimajor axis to semiminor axis of the flux rope (in a coordinate system based on an arc sweeping in latitude through the flux rope). Since the effect of spherical expansion is to increase the meridional (or θ) component of the magnetic field at the expense of the radial component, this new free parameter could be incorporated here. Models of flux ropes that fit to an elliptical geometry (e.g., Hidalgo et al. 2002b), while an improvement over cylindrical fits, do not take into account the curvature of the MC in the meridional plane. In fact, to generate a truly elliptical structure at 1 AU would require that the northern and southern flanks of the ejecta were traveling faster than lower latitude portions at just the right amount to maintain the elliptical geometry—a scenario that is unlikely to be met in any typical ambient solar wind. In spite of these limitations, force-free and non–force-free models (1) are easy to apply to in situ measurements and (2) provide the only way to infer the cloud's orientation, chirality, and radial dimension. Thus, they will likely remain an important tool for analyzing magnetic clouds for the foreseeable future. It should be emphasized, however, that such techniques apply only locally in the vicinity of the cloud. In the presence of a structured ambient solar wind, the global picture of the ejecta will likely be significantly different from that drawn from the fitted parameters. The accuracy of these fitting techniques, both in view of the results presented here and from dynamic contributions, remains to be established. We have recently begun a study using simulated time series (extracted from global MHD simulations with realistic ambient solar wind conditions) for which we know the local and global properties of the flux rope to quantify the accuracy of a variety of these fitting techniques.

In closing, we reiterate that while the techniques employed in this study are exceptionally simple, their implications for MC and ICME modeling are important. On one hand, they compel future force-free methods to include the convex-outward geometries that are an inescapable consequence of the spherical expansion of the CME and the solar wind in which it is embedded. On the other hand, they highlight the pronounced contribution of kinematic effects to CME evolution that have often been ascribed to dynamical effects.

P. R. gratefully acknowledges the support of the National Aeronautics and Space Administration (LWS Program and SEC-GI) and the National Science Foundation (the SHINE Program and the Center for Integrated Space Weather Modeling) in undertaking this study. N. U. C. would like to acknowledge support from NASA (NAG5-10881). The authors are also grateful to G. Siscoe for motivating discussions at the second Elmau CME workshop.

REFERENCES

Antiochos, S. K., Devore, C. R., & Klimchuk, J. A. 1999, ApJ, 510, 485
Bothmer, V., & Schwenn, R. 1998, Ann. Geophys., 16, 1
Burlaga, L. F. 1988, J. Geophys. Res., 93, 7217
Burlaga, L. F., Lepping, R. P., & Jones, J. A. 1990, in Physics of Magnetic Flux Ropes (Geophys. Monogr. 58; Washington: AGU), 373
Burlaga, L. F., Sittler, E. C. J., Mariani, F., & Schwenn, R. 1981, J. Geophys. Res., 86, 6673
Cargill, P. J., & Schmidt, J. M. 2002, Ann. Geophys., 20, 879
Crooker, N. U., & Intriligator, D. S. 1996, J. Geophys. Res., 101, 24343
Filippov, B. P., Gopalswamy, N., & Lozhechkin, A. V. 2001, Sol. Phys., 203, 119
Gosling, J. T. 1990, in Physics of Magnetic Flux Ropes (Geophys. Monogr. 58; Washington: AGU), 343
Gosling, J. T., McComas, D. J., Phillips, J. L., Weiss, L. A., Pizzo, V. J., Goldstein, B. E., & Forsyth, R. J. 1994, Geophys. Res. Lett., 21, 2271
Hidalgo, M. A., Cid, C., Vinas, A. F., & Sequeiros, J. 2002a, J. Geophys. Res., 106, SSH1
Hidalgo, M. A., Nieves-Chinchilla, T., & Cid, C. 2002b, Geophys. Res. Lett., 29, 15
Hu, Q., Smith, C. W., Ness, N. F., & Skoug, R. M. 2003, Geophys. Res. Lett., 30, 38
Hu, Q., & Sonnerup, B. 2002, J. Geophys. Res., 107, SSH10
Lepping, R. P., Jones, J. A., & Burlaga, L. F. 1990, J. Geophys. Res., 95, 11957
Lin, J., Forbes, T. G., Isenberg, P. A., & Demoulin, P. 1998, ApJ, 504, 1006
Linker, J. A., & Mikić, Z. 1997, in Coronal Mass Ejections: Causes and Consequences, ed. N. Crooker, J. Joselyn, & J. Feynmann (Geophys. Monogr. 99; Washington: AGU), 269
Lundquist, S. 1950, Ark. Fys., 2, 361
Marubashi, K. 1997, in Coronal Mass Ejections: Causes and Consequences, ed. N. Crooker, J. Joselyn, & J. Feynmann (Geophys. Monogr. 99; Washington: AGU), 147
Mikić, Z., & Linker, J. A. 1994, ApJ, 430, 898
Mulligan, T., Russell, C. T., Anderson, B. J., & Acuna, M. H. 2001, Geophys. Res. Lett., 28, 4417
Newkirk, G., J., Hundhausen, A. J., & Pizzo, V. J. 1981, J. Geophys. Res., 86, 5387

Odstrcil, D., Linker, J. A., Lionello, R., Mikić, Z., Riley, P., Pizzo, V. J., & Luhmann, J. G. 2002, J. Geophys. Res., 107, SSH14
Riley, P., & Gosling, J. T. 1998, Geophys. Res. Lett., 25, 1529
Riley, P., Gosling, J. T., & Pizzo, V. J. 1997, J. Geophys. Res., 102, 14677
Riley, P., Linker, J. A., Mikić, Z., Odstrcil, D., Pizzo, V. J., & Webb, D. F. 2002, ApJ, 578, 972
Riley, P., Linker, J. A., Mikić, Z., Odstrcil, D., Zurbuchen, T. H., Lario, D. A., & Lepping, R. P. 2003, J. Geophys. Res., 108, SSH2
Russell, C. T., & Mulligan, T. 2002, Adv. Space Res., 29, 301
Schmidt, J., & Cargill, P. J. 2001, J. Geophys. Res., 106, 8283
Suess, S. T. 1988, J. Geophys. Res., 93, 5437
Titov, V. S., & Demoulin, P. 1999, A&A, 351, 707
Vandas, M., Odstrcil, D., & Watari, S. 2002, J. Geophys. Res., 107, SSH2